

T. B. McCord and D. P. Cruikshank
University of Hawaii
Honolulu, Hawaii 96822

1. INTRODUCTION

Near infrared spectrophotometry has vastly increased our knowledge of the composition and structure of asteroids, satellites and planetary surfaces over the past ten years. In this article we will attempt to summarize the most recent comprehensive results. We will emphasize the interpretations and present only examples of the data.

At visible and near infrared wavelengths the radiation received from solar system objects is passively scattered solar radiation. At longer wavelengths thermal emitted radiation dominates. (Figure 1 shows the two radiation components for the lunar case.) The wavelength at which the two components contribute equally is about 2.5 μm for the moon's sub-solar point. For Mercury this wavelength is near 1.9 μm and for the colder outer solar system objects the wavelength is farther into the infrared.

At certain energies associated with the visible and near-infrared wavelengths, electronic and molecular transitions occur which result in absorption of solar radiation by surface material. Spectra of solar radiation reflected from surfaces of solar system objects show these absorptions. At visible and near infrared wavelengths longward to about 2.5 μm , transitions of d-shell electrons in transition metal ions and electron exchange between ions are mainly responsible; iron ions are particularly important. Molecular oscillations result in absorptions longward of about 1 μm , with H₂O and OH being most important.

The electronic absorptions occur at energies controlled by the particular ion present and by the electric field the ion experiences. These properties generally define mineralogy. Similar interpretations can be made of certain molecular absorptions; ice, for example, is a mineral.

In this review we first consider the relatively nearby objects which can be resolved into several individual surface elements by

present techniques of remote sensing. Progress has been made in mapping the surface compositions of some of these bodies, and the work continues with large telescopes at high-quality ground-based observatories. In a later section we consider the smaller and more distant solar system objects which cannot be resolved into surface elements and for which global, or hemispheric, averages of surface composition are revealed by the techniques of remote sensing.

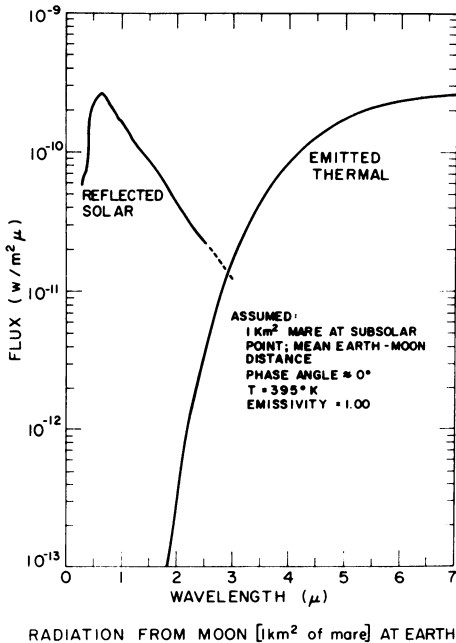


Figure 1. The radiation received from the moon is shown for the extended visible and near- to mid-infrared spectral regions. The two radiation components, reflected and emitted, are obvious.

2. THE MOON AND TERRESTRIAL PLANETS

Mercury

Ground-based telescopic observations of Mercury are difficult to make because Mercury is close to the sun and only appears in the sky during the day or near the horizon at twilight, when the sky is still bright and line-of-sight air mass is great. McCord and Adams (1972a,b) reported a possible weak absorption in the Mercury spectrum near $0.95\ \mu\text{m}$, but the data were of insufficient quality to be certain. Vilas and McCord (1976) later found no feature with greater contrast than a few percent. Tepper and Hapke (1977) reported a weak absorption band near $1\ \mu\text{m}$, but as in the earlier measurements, the feature was about the same strength as the uncertainty in the measurement.

More recently, a continuously spinning CVF spectrometer (McCord et al., 1978) was used to obtain the Mercury spectrum between 0.65 μm and 2.5 μm (McCord and Clark, 1979). The reflectance was calculated and is shown in Figure 2 for three different observing sessions.

The Mercury reflectance spectrum shows a continuous increase in reflectance from visible to infrared wavelengths. A very similar continuum is evident for lunar surface material, as measured through the telescope (Figure 2). With the possible exception of the dark side of Saturn's satellite Iapetus, no other objects in the solar system so far observed have similar spectral reflectance.

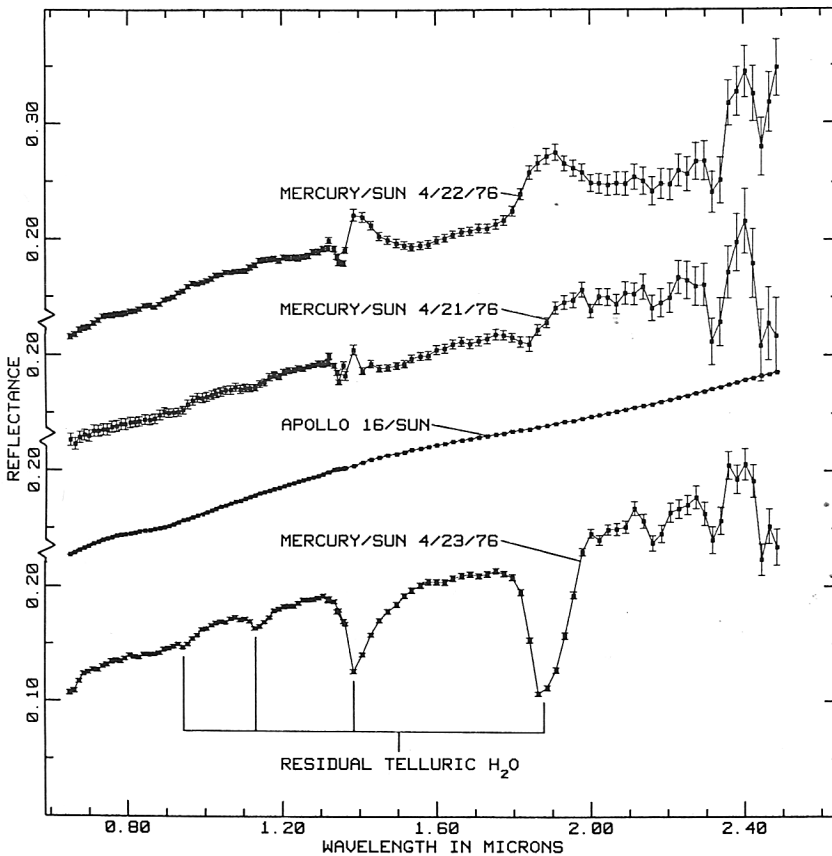


Figure 2. Spectral reflectance of Mercury for the three nights on which observations were made. The stronger telluric H_2O bands, which were not completely removed by extinction corrections, are noted. The spectral reflectance of Apollo 16 site soil as measured in the laboratory is shown for comparison. This and Figures 3 and 4 from McCord and Clark (1979).

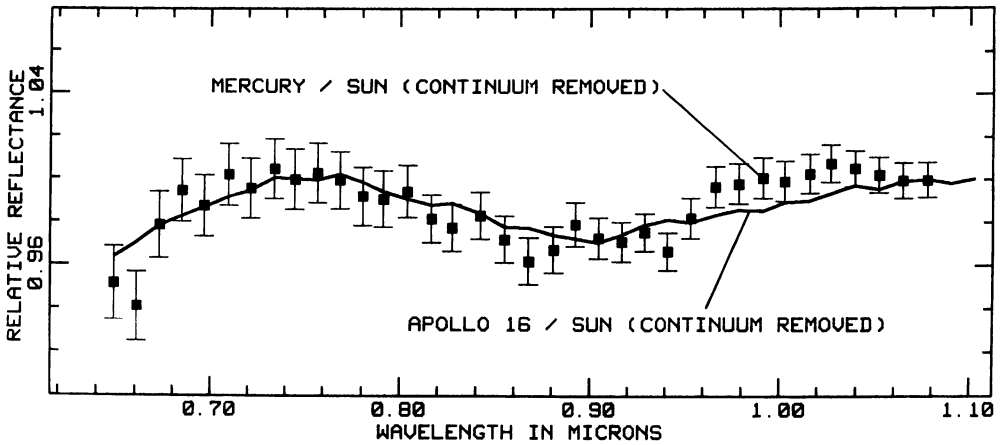


Figure 3. Spectral reflectance of Mercury (points) and of Apollo 16 soil measured in the laboratory [Adams and McCord, 1973] (continuous line) are shown overlaid. A straight line continuum slope fitted at 0.745 and 1.078 μm has been removed from each spectrum.

The weak reduction in reflectance between 0.75 and 0.95 μm is of particular interest, and it is more clearly shown in Figure 3. The continuum of the reflectance spectrum in this spectral region has been removed from both the Mercury and Apollo 16 site spectra by dividing by a straight line fitted to the spectra at 0.745 μm and 1.078 μm .

As originally proposed by McCord and Adams (1972a, b), this very weak and broad absorption is probably due to d-shell electronic transitions in Fe^{2+} ions either in a mafic mineral, probably pyroxene, in glass, or in both. The band center spectrum is located at 0.89 μm , as seen in Figure 4, according to a Gaussian band-fitting calculation. This band position suggests an orthopyroxene as the major mafic mineral affecting the spectrum and tends to rule out glass.

The absorption feature between 0.75 and 0.95 μm in the Mercury spectra is nearly the same strength, but the band center is at slightly shorter wavelengths in comparison to that in the spectrum of lunar highlands Apollo 16 site soil shown in Figures 2 and 3. The absorption band is weaker than for most lunar maria and all lunar fresh crater material. The weak band strength could be due to the amount of Fe^{2+} ions present or to an opaque phase reducing the spectral contrast. The latter case would result in a very low albedo soil, much lower in albedo than for Mercury (Hapke et al., 1975). Thus it was argued (McCord and Clark, 1979) that the average Mercury soil has about the same amount of Fe^{2+} as Apollo 16 site lunar highland soil, which averages about 5.5% FeO (Taylor, 1975; Rose et al., 1975).

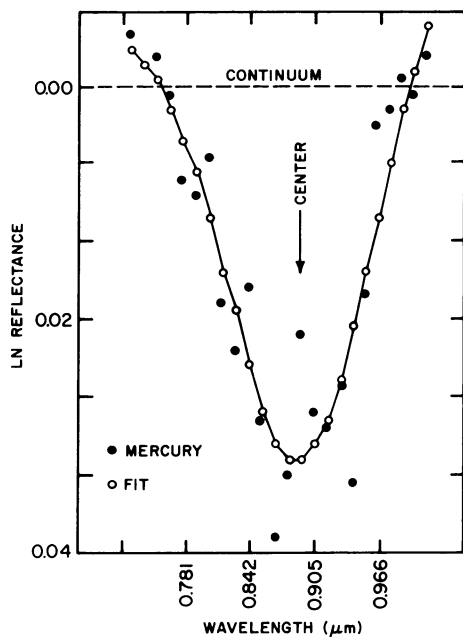


Figure 4. The Mercury reflectance spectrum segment shown in Figure 3 (solid circles) is shown computer-fitted by a single Gaussian curve (open circles). Band depth is 4%, band center is $0.890 \mu\text{m}$, and bandwidth is $0.165 \mu\text{m}$ using the continuum shown.

The presence of Fe^{2+} in the soil of Mercury is important, since it suggests that Mercury surface soil is not reduced completely and all the iron is not in metallic form. In the case of Mercury, it is difficult to attribute a soil rich in oxidized Fe to primary condensation processes, because oxidized iron does not appear in quantity in the projected condensation sequence until temperatures far below those envisioned for condensation of average Mercury material. A more likely explanation is that a Mercury crust rich in iron-bearing pyroxene resulted from familiar processes leading to basaltic surface volcanism.

Hapke et al. (1975) used Mariner 10 images in two spectral bands centered at $0.355 \mu\text{m}$ and $0.575 \mu\text{m}$ to map albedos and colors over portions of the Mercury surface. The higher albedos are similar to those for lunar highlands, and the lower albedos are somewhat higher than for lunar maria. The color maps showed differences and boundaries. Apparently fresher material exposed near craters is bluer in color as it is in the lunar case.

The Moon

Spectrophotometry of the lunar surface has been an area of active research since early in this century, when it was realized that the color of a material was related to its composition. Until 1965 the observations were confined to the visible spectral region, where spectral coverage was not sufficient to define electronic absorption features. Consistency of the measurements with volcanic materials was often mentioned, but conclusive evidence was missing. Perhaps most important was considerable evidence that there are surface units of differing composition with sharp boundaries. A review of this early work is given by McCord (1968).

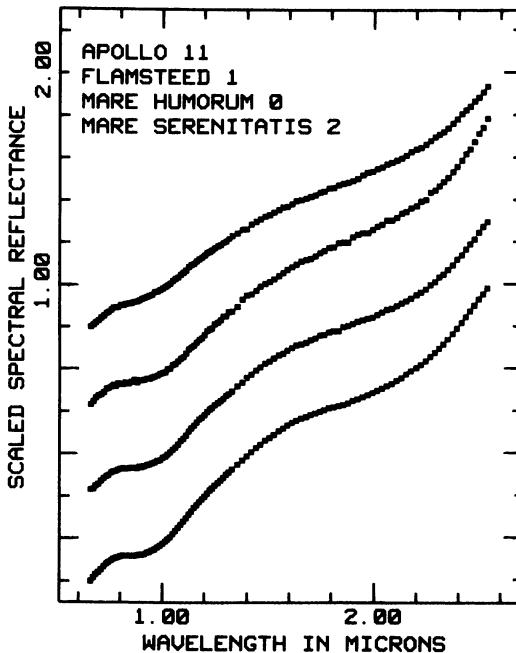


Figure 5. The spectral reflectance for several lunar areas is shown (McCord et al. 1980). Note the variety of spectrum slopes and the different intensities of the Fe^{2+} bands near 1 μm and 2 μm .

Near infrared observations of lunar areas began in the 1960s as the technology developed. Early measurements revealed little compositional information because of insufficient photometric precision (see McCord et al. 1980, Figure 1). Later differential measurements of lunar reflectance for area-pairs in the 0.7 μm to 2.5 μm spectral region showed structure near 1.0 μm indicating the presence of Fe^{2+} electronic transition bands in mafic minerals.

The spectral structure varied from area to area suggesting mineralogic variations. Adams and McCord (1970) compared new telescopic reflectance spectra of lunar areas with laboratory spectra of lunar samples from Apollo 11 to show Fe^{2+} absorption features near $0.95 \mu\text{m}$ in both spectra. The $0.95 \mu\text{m}$ absorption was attributed to Fe^{2+} in the mafic mineral pyroxene, a major constituent of basalt. McCord et al., (1972) reported a number of lunar reflectance spectra to $1.1 \mu\text{m}$ defining the Fe^{2+} absorption feature and showing the variation of it and the spectra continuum with lunar terrain type. Since then a large number of visible and very near infrared reflectance spectra of lunar areas have been collected and used (e.g. Pieters and McCord, 1976; Pieters, 1978; Pieters et al., 1980) to derive information on the composition and structure of the lunar surface. But it was clear that measurements beyond $1.0 \mu\text{m}$ would provide additional information.

Recently, McCord et al. (1980) obtained reflectance spectra of high photometric precision of small lunar areas between $0.65 \mu\text{m}$ and $2.5 \mu\text{m}$, including through the regions of the terrestrial water bands near $1.4 \mu\text{m}$ and $1.9 \mu\text{m}$ (Figure 5). Several electronic absorption features are revealed in the spectra; in particular, bands due to pyroxene and plagioclase are present. Computer analysis of the bands (in these very precise data) provides quantitative mineralogical information. Figure 6 demonstrates the removal of the reflectance continuum and the quantitative specification of the bands.

The quantitative information on absorption bands can be used with laboratory studies of the optical properties of lunar and terrestrial materials to develop quantitative mineralogical information about small areas on the lunar surface (McCord et al., 1980). For example, consider the spectrum for a ten-kilometer area in the crater Aristarchus (Figure 7). The band positions are $0.96 \mu\text{m}$ and $2.26 \mu\text{m}$ for pyroxene and $1.28 \mu\text{m}$ for the mineral plagioclase.

Adams (1974) has explored in the laboratory the optical properties of pyroxene and has shown that the positions of the two bands change in a regular way with the mineral composition (Figure 8). The bands move to longer wavelengths (lower energies) as the iron and calcium content increases and the crystal structure expands. The position of the Aristarchus bands on the plot indicates the presence of a pyroxene of augite composition. Plots of Fe and Ca content versus band positions have been made by Adams (1974) and they can be used to show that the Aristarchus augite has $25 \pm 5\% \text{ Ca}/(\text{Ca} + \text{Mg} + \text{Fe})$. This composition is consistent with a mare basalt. Since the crater is located in a region of apparently only thin mare covering over underlying terra material, one would expect to sense terra material in the crater. Perhaps the mare is deeper than thought at this place or a unit of mare material became incorporated in the crater so that it composed the floor of the crater. More spectra are being obtained around the crater to map the ejecta blanket composition and work out the structure of the crater and the lunar surface in the crater region.

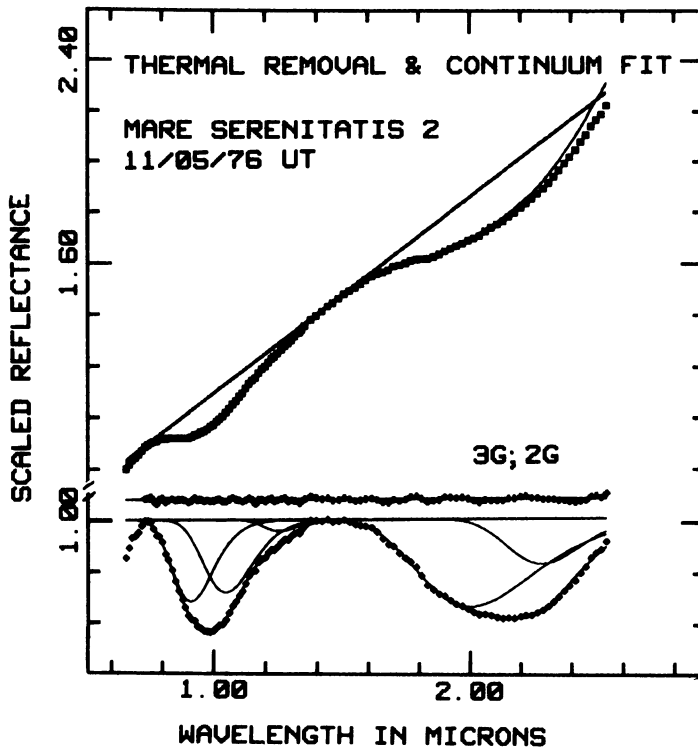


Figure 6. The method of continuum removal and absorption band analysis is illustrated here using the spectrum for an area in Mare Serenitatis (McCord et al. 1980). The line spectrum in the upper plot is the reflectance with the thermal emission component of radiation; the point spectrum has the thermal contamination removed.

From the spectroscopic studies it has been possible to determine relationships between measurements in a few spectral bands and certain compositional properties. These optical properties and thus compositional properties can then be mapped in two dimensions. An example is the map of basalt types developed for the geological study of the

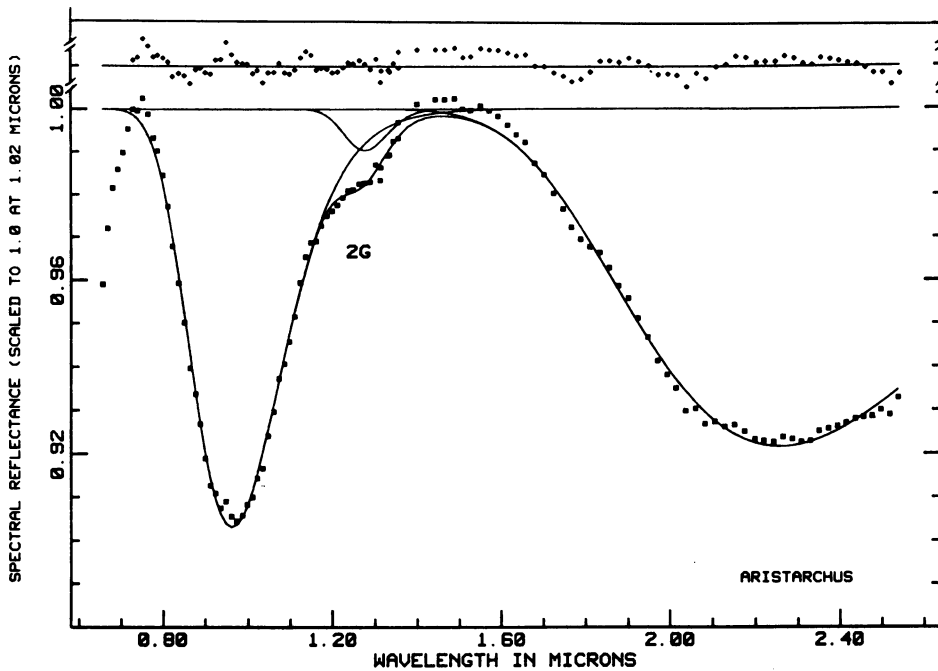


Figure 7. The spectrum for the crater Aristarchus is shown with the continuum removed and three gaussian functions fitted (McCord et al., 1980). The bands at 0.96 μm and 2.26 μm are due to pyroxene and augite; the band at 1.28 μm is due to plagioclase.

Flamsteed region of Oceanus Procellarum (Figure 9) (Pieters et al., 1980). This map was developed using a relationship between titanium content in the lunar surface material and the slope of the reflectance spectrum between 0.40 μm and 0.56 μm (Charette et al., 1974; Pieters, 1978). Titanium content is a good basis on which to distinguish lunar maria basalt types. The map in Figure 9 was produced by obtaining digital photometric images of lunar regions through filters with bandpasses centered at 0.40 μm and 0.56 μm (McCord et al., 1976, 1979). The calibrated images are divided, pixel by pixel, to produce a map of reflectance spectrum slope and thus of titanium. Other regions of the moon have been studied this way (e.g. Johnson et al., 1977a,b; Head et al., 1978) and the number of studies and compositional-optical property relationships is expanding.

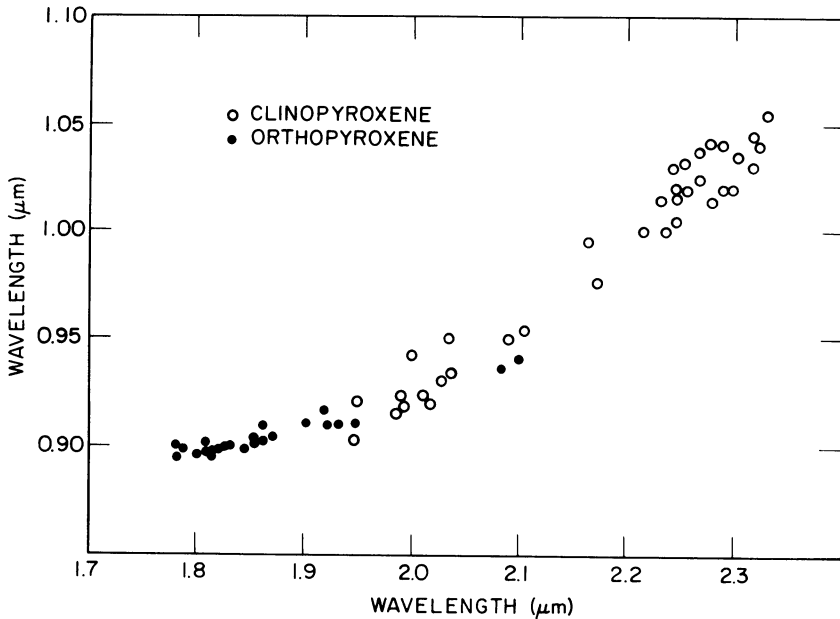


Figure 8. The mineral pyroxene has two strong Fe^{2+} bands in its diffuse reflectance spectrum. This plot shows the shift in wavelength of these two bands as the pyroxene composition changes (Adams, 1974).

Mars

To a visual observer Mars is red with spots of high and low albedo. The distinctive red color led early observers to suggest that iron oxide is a constituent of the surface material. This has been repeatedly confirmed by detailed studies of the Mars spectrum and considerably more compositional information also has been derived. Spectroscopic studies and compositional interpretation of Mars have been reviewed recently (Singer et al., 1979). The reader is referred to that review for a current, detailed discussion.

Visible and near-infrared (0.3 - 2.6 μm) reflectance spectra of the martian surface have been obtained primarily from earth-based telescopic observations, and multispectral images have been obtained both from spacecraft and earth-based observations. Observations in this wavelength region have confirmed the bimodal albedo distribution of surface materials first observed visually. All spectra of Mars are characterized by strong Fe^{3+} absorptions from the near-UV to about 0.75 μm . Darker regions show this effect to a lesser degree, and are interpreted to be less oxidized materials. In addition, dark areas have Fe^{2+} absorptions near 1.0 μm , attributed primarily to olivines and pyroxene. There is evidence at infrared wavelengths for highly

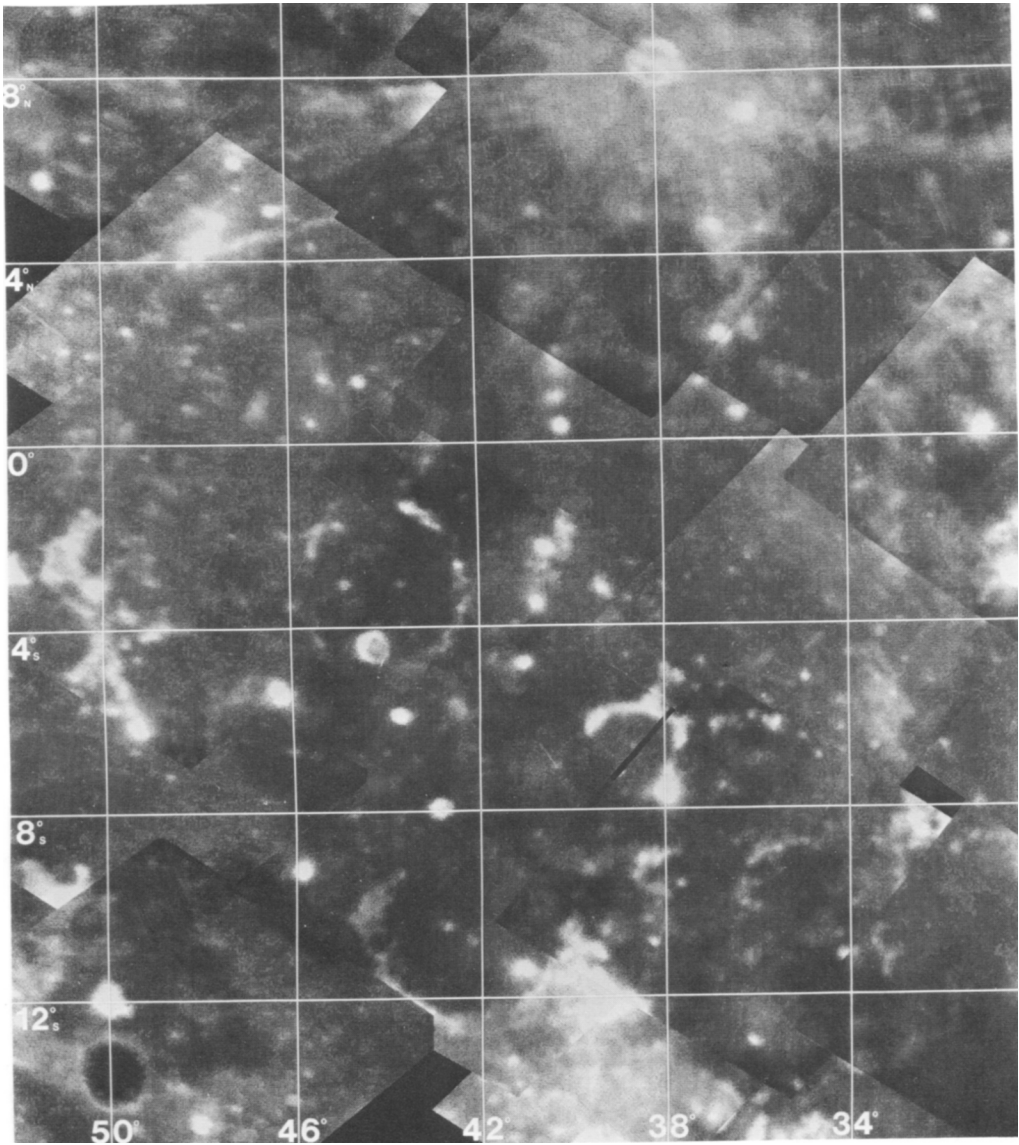


Figure 9a. Multispectral maps of the Flamsteed region of the Moon. These maps are mosaics of digital images acquired using groundbased telescopes. This is an image mosaic of the Flamsteed region made through a $0.56 \mu\text{m}$ filter; grey tones correspond to albedo. This and Figure 9b from Pieters et al. (1980).

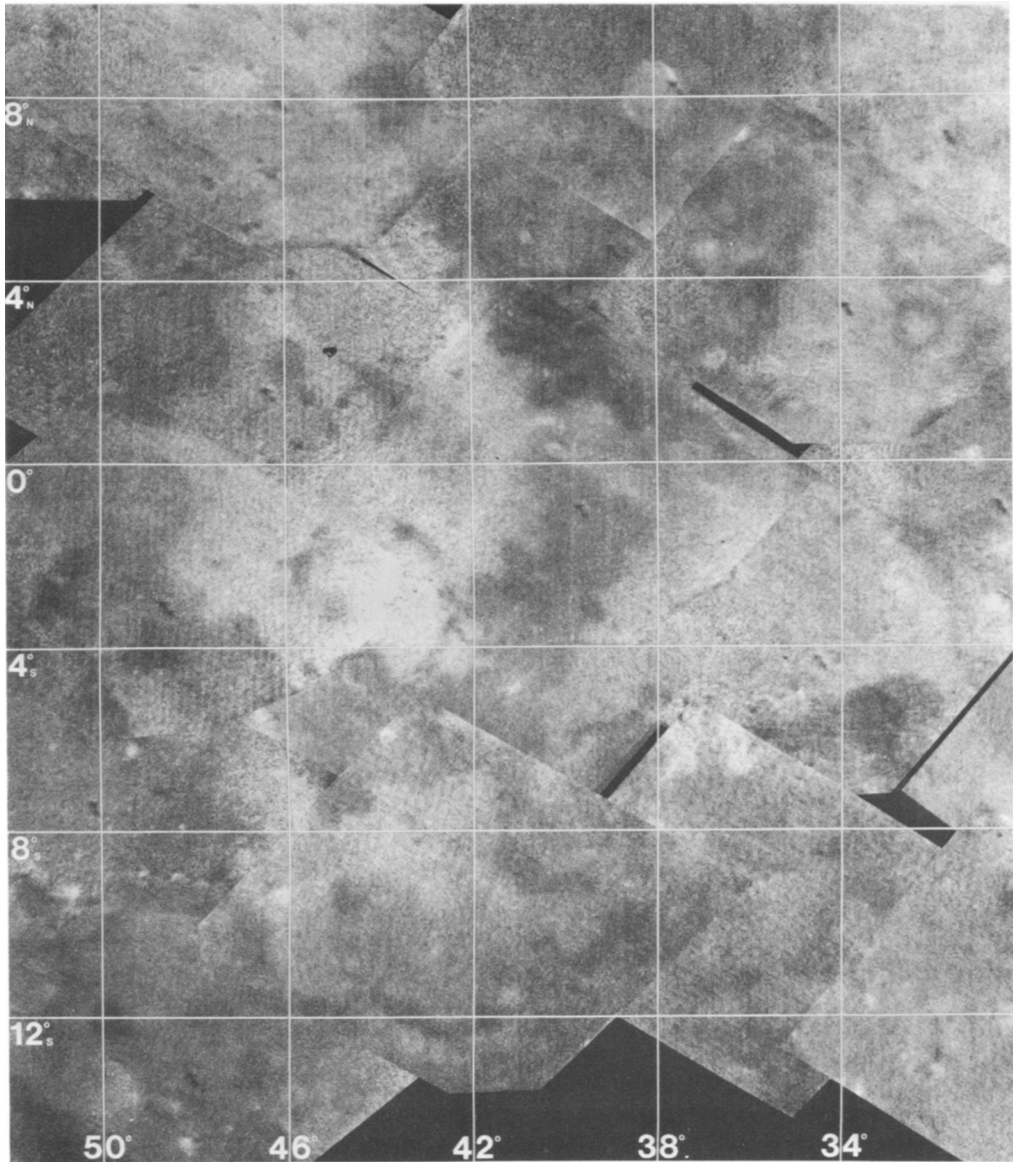


Figure 9b. Grey tone representation of the areal distribution of the reflectance ratio $0.40/0.56 \mu\text{m}$. This figure is produced by dividing images made at 0.40 by images made at $0.56 \mu\text{m}$ and contrast enhancing the result. Bright indicates a high UV/VIS ratio.

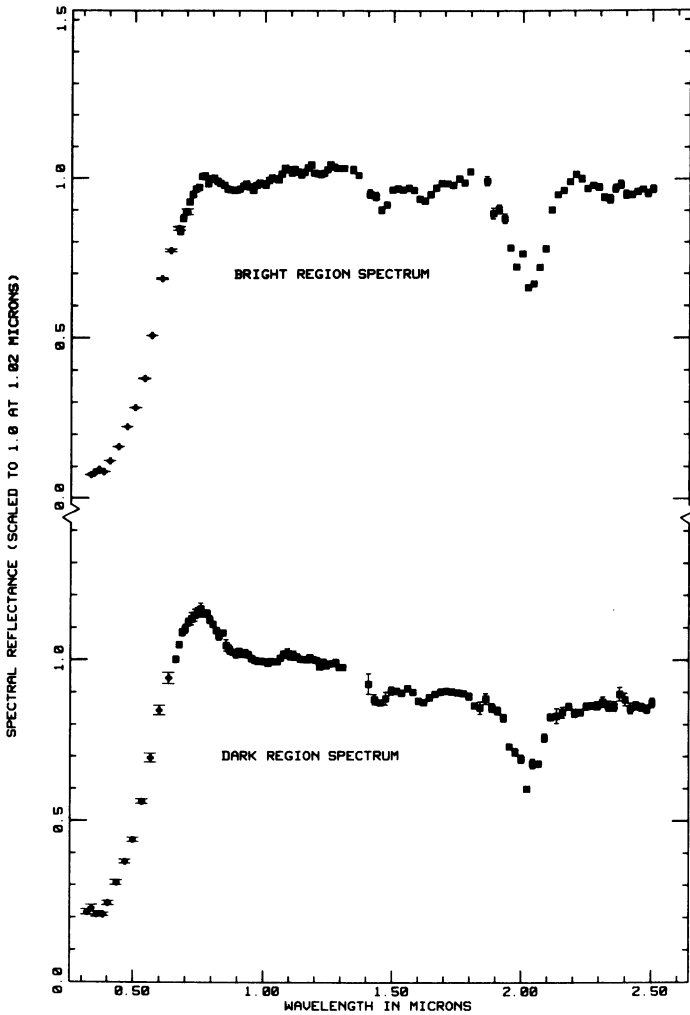


Figure 10. Representative bright and dark region reflectance spectra, scaled to unity at 1.02 μm . The bright region spectrum (top) is composed of an average of the brightest areas observed. The dark region spectrum (bottom) is a composite of data from two nearby locations in Iapygia. This and Figure 11 from Singer et al. (1979).

desiccated mineral hydrates and for H_2O -ice and/or adsorbed H_2O . Observations of the north polar cap show a strong H_2O -ice spectral signature but no spectral evidence for CO_2 -ice, while only CO_2 -ice has been identified in spectra of the south polar cap. The brightest materials on Mars show greater mineralogic variability and are thought to be closer in petrology and physical location to their parent rock. At present the best model for the dark materials is a somewhat

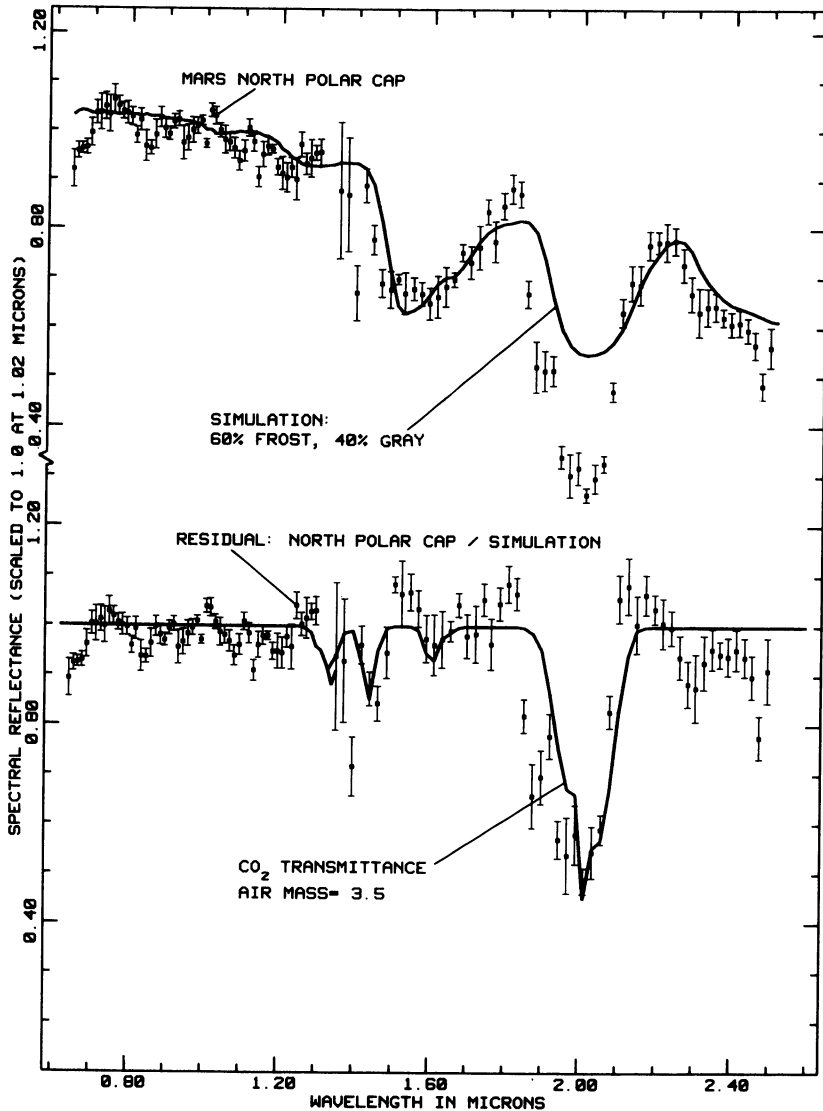


Figure 11. The martian north polar cap spectrum compared with an additive simulation of ice and a grey material (top). The ratio of the polar cap spectrum to the simulation is then compared with the expected CO₂ martian transmittance (bottom) [from McCord et al., 1979].

oxidized basaltic or ultramafic rock, regionally variable in composition and details of oxidation. The bright materials appear to be finer-grained assemblages of primarily highly oxygen-sharing desiccated mineral hydrate, some ferric oxides, and other less major constituents,

including a small amount of relatively unaltered mafic material. The bright materials seem likely to be primary and/or secondary alteration products of the basaltic or ultramafic dark materials.

Representative Mars spectra are shown in Figure 10 and 11. Examples of visible spectra are given in Singer et al. (1979).

Reflectance observations from spacecraft consist mainly of multi-spectral images from Viking orbiters and landers. Soderblom et al. (1978) have prepared three-color photometric maps for a large portion of the planet between latitudes 30° N and 60° S from VO 2 approach images ($L_S = 105^{\circ}$). These have good spatial resolution (10-20 km) but limited spectral coverage and resolution (three broad bands: $0.45 \pm 0.03 \mu\text{m}$, $0.53 \pm 0.05 \mu\text{m}$, and $0.59 \pm 0.05 \mu\text{m}$). Soderblom and others are preparing additional multispectral maps using Viking orbital images of selected regions and at higher spatial resolution (L. A. Soderblom, personal communication, 1979). Viking lander cameras are capable of taking images in six spectral bandpasses from 0.4 to 1.0 μm . Huck et al. (1977) developed a technique for transforming these six brightness values into an estimate of spectral reflectance. These data are being used successfully for determining color differences and properties of the surface at the two landing sites (Evans and Adams 1979; Strickland 1979). As with orbital data, repeat coverage is available throughout a martian year, permitting monitoring of variations in surface optical properties (Guinness 1979).

3. DISTANT, UNRESOLVED OBJECTS

The remote sensing of the compositions of solar system objects which are too small or distant to be resolved into a significant number of surface elements has progressed along several lines. Photometry and polarimetry of these objects have given information on their surface microstructures, and virtually all of those bodies not having atmospheres are found to have surface microtextures indicative of a regolith of finely divided material, whether composed of rocky/dusty powder or frozen volatiles (water or methane ice). Spectrophotometric investigations in the photovisual region (0.2 - 1.0 μm) have revealed specific absorptions in the iron-bearing minerals, as already described, and slopes, usually upward toward the red, of varying degrees and indicative of mineral absorptions in the violet and blue spectral region. This work, when extended further to the near infrared (1.0 - $\sim 5 \mu\text{m}$), where the light received from the objects is reflected sunlight, shows additional stronger absorption bands characteristic of various frozen volatiles and minerals. It is in this spectral region where the greatest amount of diagnostic compositional information has been obtained in recent years, both from spectrophotometry, spectroscopy, and filter photometry. In this section we will review the major results of near infrared studies of the outer planetary satellites and Pluto.

Asteroids

Almost all of the available information on the chemistry of the asteroids, as well as that on their physical states, has been developed in the past decade, and this knowledge has been summarized in two books (Gehrels, 1971, 1979). Photoelectric photometry (UBV) has produced colors for over 700 asteroids (cf. Bowell and Lumme, 1979). These colors have been plotted on a B-V, U-B diagram to show clumpings. These clumpings, when used with albedo and spectra, have been used to infer statistical properties of the asteroids. A major advantage of the UBV measurements is that they can be made for fainter asteroids than those for which full spectra can be obtained.

The reflectance of an asteroid surface as a function of wavelength from UV to the IR (where thermal emission becomes important near 5 μm) is the property found to be most directly indicative of surface composition. Therefore a great deal of effort has gone into the acquisition and interpretation of such data during the past decade. Since the first observations of the spectral reflectance of Vesta and the discovery that its surface contained basaltic material (McCord et al., 1970), reflectance spectra between 0.35 μm and about 1.1 μm have been obtained for over 277 asteroids (cf. Chapman and Gaffey, 1979).

Inspection of the representative spectra in Figure 12 shows that a wide variety of spectral features is evident, indicating heterogeneous composition. The mineral assemblages detected on asteroids are generally similar to meteoritic minerals. Mafic silicate minerals (pyroxene and olivines), opaques and metals are the major constituents (cf. Gaffey and McCord, 1978, 1979).

Spectra in the near infrared spectral region to 2.5 μm (reviewed by Larson and Veeder, 1979) of a few asteroids have confirmed the presence of pyroxene and have demonstrated the existence of plagioclase. Spectrophotometry of Ceres in the 3.0 μm region revealed H₂O absorptions suggesting hydrated minerals (Lebofsky, 1978). A few other asteroids appear to show a band of adsorbed H₂O, but these measurements are still preliminary. The continued exploration of the asteroids by spectrophotometry will be a major endeavor for the next decade. As the statistical sample improves, more detailed studies of compositional families and their possible relationship to dynamical families of asteroids can proceed. One major goal of this work is the search for parent bodies of the meteorites found on Earth, and another is the search for asteroidal sources of natural materials of potential economic importance (Gaffey and McCord, 1977a,b).

The Galilean Satellites

The surface compositions of the Galilean satellites have been thoroughly reviewed by Sill and Clark (1981) in the context of ground-based observations and the results of Voyager 1 and 2. Before the Voyager discovery of active volcanism on Io, absorption bands at 4.08 μm

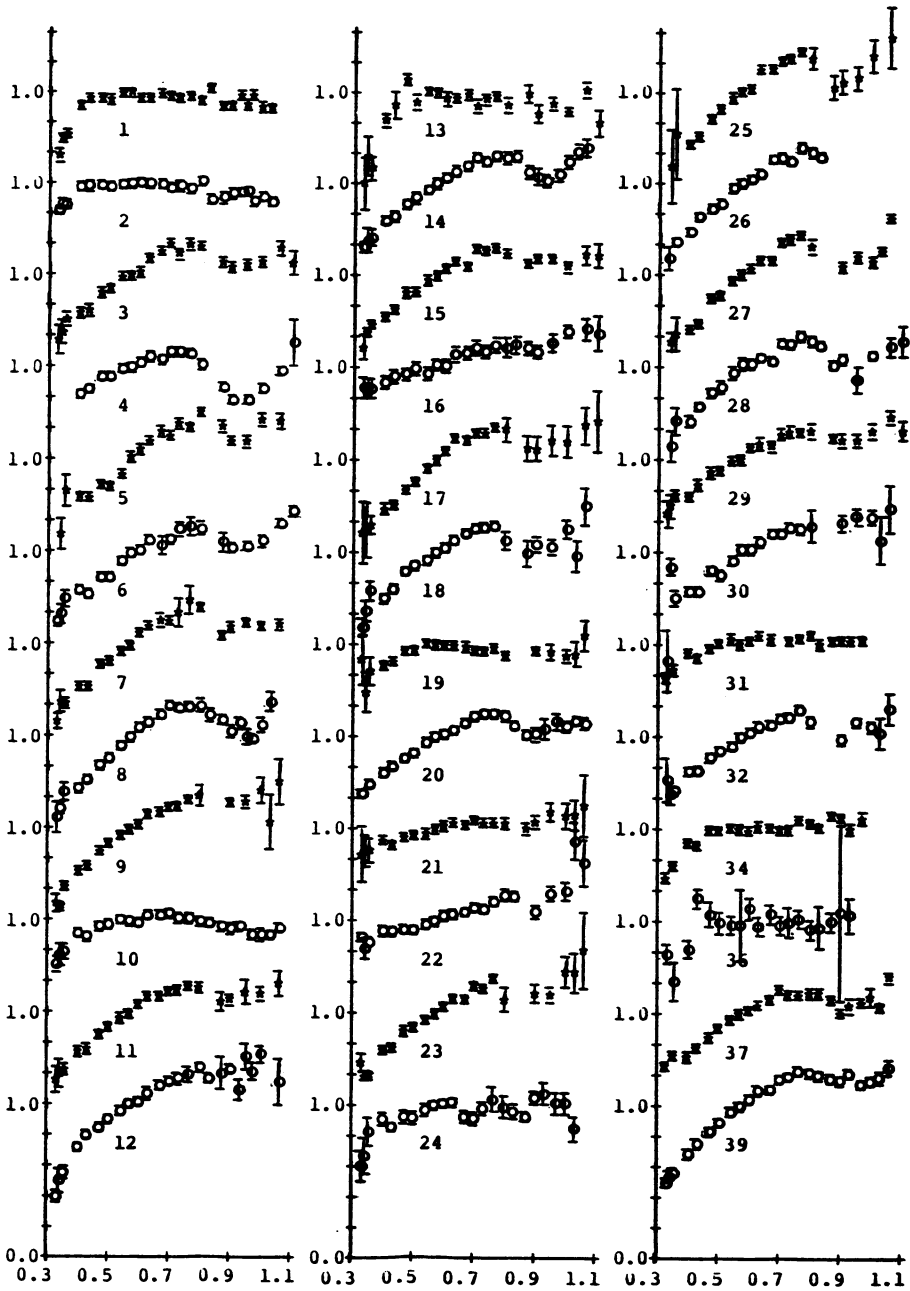


Figure 12. The spectral reflectance for a selection of the brighter asteroids is shown here to illustrate the variety of curve types (Chapman and Gaffey 1979).

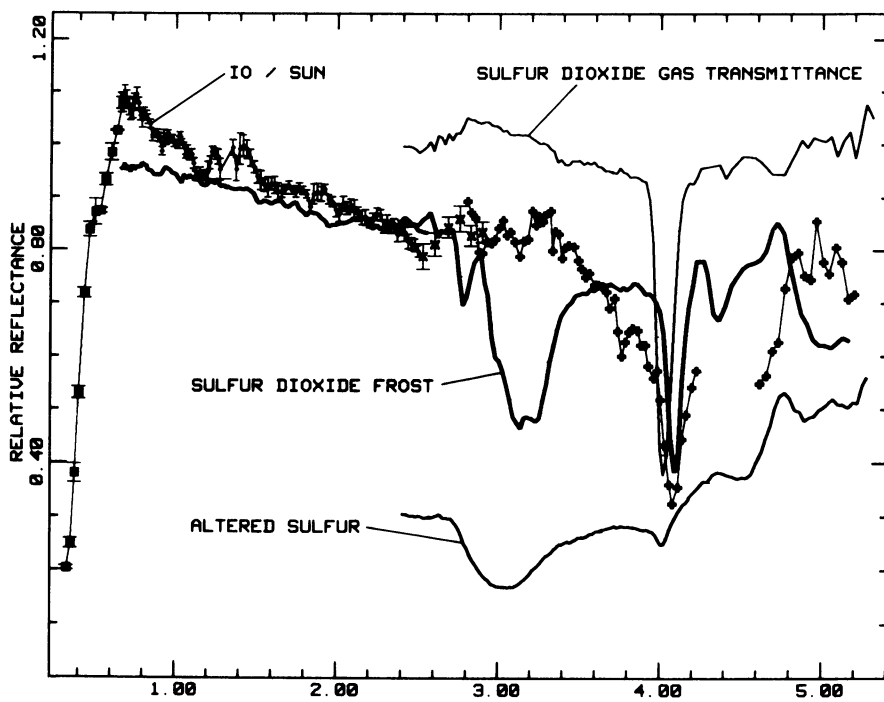


Figure 13. The reflectance spectrum of Io, with laboratory spectra of SO_2 gas and frost and a sample of a sulfur allotrope. The absorption at $4.08 \mu\text{m}$ in the Io spectrum is attributed to SO_2 frost on the basis of this comparison. From Fanale et al. (1979).

and nearby were found from ground-based spectra (Cruikshank et al. 1978, Fink et al. 1978, Cruikshank 1980a) and identified as SO_2 frost (Fanale et al. 1979). The discovery of active volcanism that quickly followed this identification explained the origin and persistence of the frost in the intense radiation field characteristic of the surface of Io. Figure 13 shows the spectrum of Io with SO_2 gas and frost, plus a solid allotrope of sulfur. Additional studies of Io from Voyager data and from spectra in the short wavelength region of the spectrum have given evidence for extensive surface deposits of numerous temperature-sensitive allotropes of sulfur (Sill and Clark 1981) as well as the SO_2 frost. In addition to frost, gaseous SO_2 was found in localized regions on the satellite with the Voyager spectrometer which revealed an absorption band at $7.35 \mu\text{m}$ (Pearl et al. 1979).

Infrared reflectance studies of the Galilean satellites began with Kuiper (1957) whose initial results in the $1\text{--}2.5 \mu\text{m}$ region led him to propose that water frost occurs on Europa and Ganymede. Moroz (1965) obtained better data in the same spectral region and reached the same conclusion, but the identification gained acceptance only when telescopic

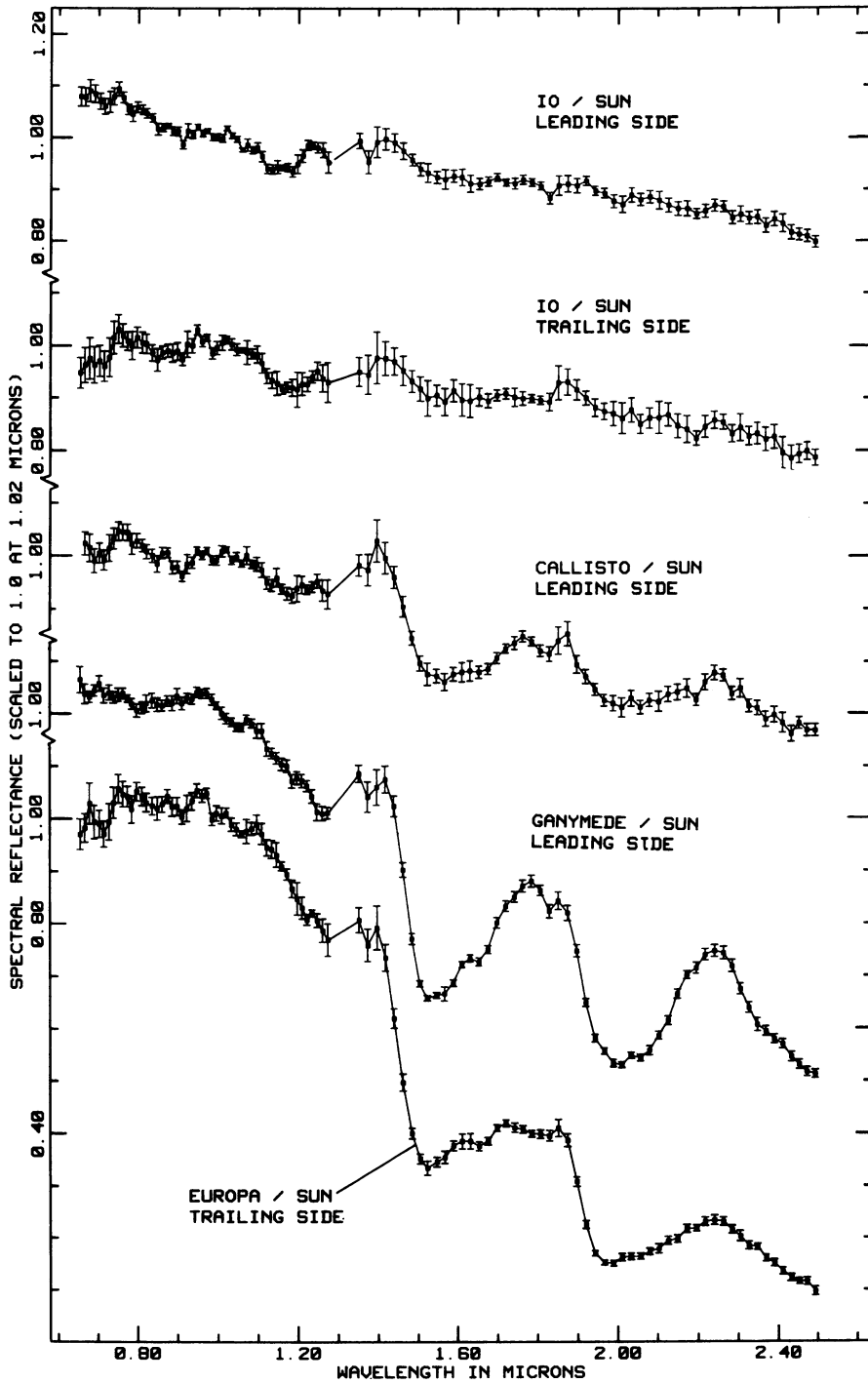


Figure 14. Reflectance spectra of the Galilean satellites, from Clark, and McCord (1980).

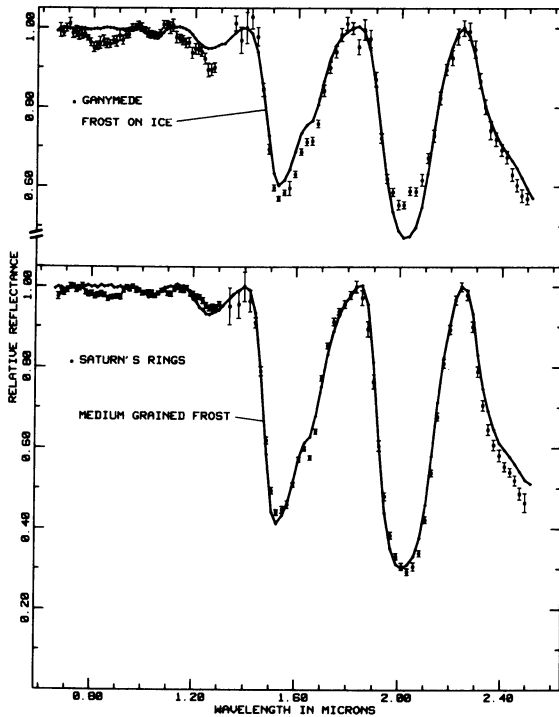


Figure 15. Infrared spectra of Ganymede and Saturn's rings with continua removed for comparison of apparent band depths. From Clark (1980).

data of high quality and better frost data than had previously appeared were presented by Pilcher et al. (1972) and Fink et al. (1973). These early results were of particular importance for Europa and Ganymede, which showed strong absorptions due to water frost in the 1-2.6 μm region, and gave only hints that some frost might be present on Callisto. The work of Clark and McCord (1980) revealed with certainty the weaker frost bands in the spectrum of Callisto, and in his analysis of all three water-frost bearing satellites, Clark (1980) showed that Ganymede's surface is about 90 percent covered with water frost, and that of Callisto about 30 to 60 percent. He notes that "The surface of Europa has a vast frozen water surface with only a few percent impurities." Those impurities, more abundant on Callisto and Ganymede, appear to consist of silicate material having reflectance spectra typical of minerals containing Fe^{3+} , and the material is intimately mixed with the frost. While the interpretation by Clark (1980) is based primarily upon ground-based spectroscopic observations in the near infrared, it is consistent with the morphological structures and distribution of albedo features observed on the Voyager images of the satellites. The best spectrophotometric data for Europa, Ganymede, and Callisto, together with water frost and ice comparisons, are shown in Figures 14, 15, and 16.

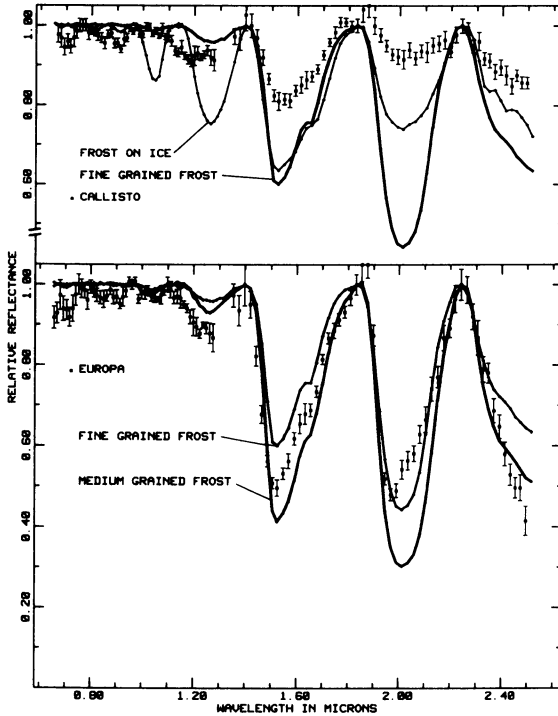


Figure 16. Reflectance spectra of Callisto and Europa with continua removed for comparison of apparent band depths. From Clark (1980).

The Small Satellites of Jupiter

There are three known satellites interior to Io. J5, Amalthea, was discovered in the last century, but only with the Voyager studies of the Jupiter system has much been learned about it. Two other small satellites, J14 and J15, were discovered with the imaging system of the Voyagers. Rieke (1975) measured thermal radiation from Amalthea, and with his data and photoelectric photometry it was possible to ascertain that the surface geometric albedo of the satellite is on the order of 5 percent, making it a member of the large family of dark objects in the outer solar system. Studies of the Voyager images and photometry by Thomas and Veverka (1981) show that Amalthea is a very irregular object in shape, about 270 x 165 x 150 km, and that its surface apparently has been contaminated by material from Io, particularly sulfur. Its bulk composition cannot, therefore, be determined from studies of its altered surface. There is no compositional information on J14 and J15, nor are there any infrared observations of any kind relevant to these objects.

In the context of the small interior satellites of Jupiter we note that infrared reflectance observations of the ring of Jupiter at 2.2 μm have been reported by Becklin and Wynn-Williams (1979); these data

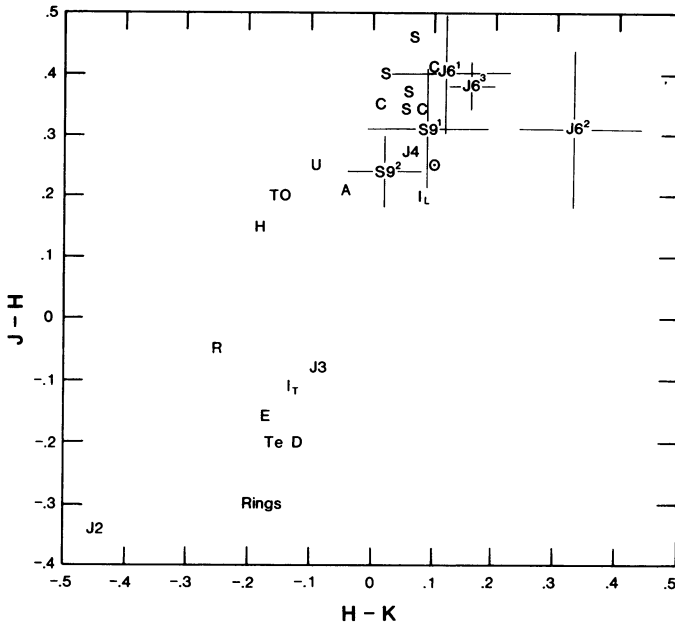


Figure 17. JHK color diagram for small solar system bodies. Key: J2 = Europa, J3 = Ganymede, J4 = Callisto, R = Rhea, E = Enceladus, Te = Tethys, D = Dione, I_T = Iapetus (trailing hemisphere), I_L = Iapetus (leading hemisphere), Rings = Saturn's rings, H = Hyperion, S9 (with superscripts) = independent observations of Phoebe, J6 (with superscripts) = independent observations of Himalia, A = Ariel, U = Umbriel, T = Titania, O = Oberon, C = C-type asteroids, S = S-type asteroids. From Degewij et al. (1980b).

together with crude spectral data in the $2\text{-}\mu\text{m}$ region by Becklin and Neugebauer (in preparation) suggest that the ring particles are of low albedo and that the reflectance is relatively flat in the narrow spectral region studied. Particles of ice or ice-covered dust grains are unlikely because of the high density of energetic particles in the region close to Jupiter; the outer edge of the ring lies at $1.81 R_J$.

The satellites exterior to the Galilean satellites, of which eight are presently known with certainty, comprise two dynamical groups. One, at $\sim 164 R_J$ has orbital inclinations on the order of 27° , and the other at $\sim 322 R_J$ with $i \sim 150^\circ$; the orbits of the Galilean and interior satellites are nearly circular with negligible inclination to the planet's equatorial plane. UBVR photometry of J6 and J7 (in the first group) and J8 (second group) and infrared radiometry of J6 and J7 indicate low geometric albedos and reflectance similar to C-type asteroids (Degewij and van Houten 1979; Cruikshank et al. 1981; Degewij et al.

1980a,b). There is spectrophotometric evidence (Smith et al. 1981) that J9 has a steep red slope in the photovisual spectral region, as do J6, J7, and J8, suggesting that these objects similarly have low albedos with dusty (as opposed to icy) surfaces, but that some differences in the surface mineralogies may occur.

Infrared observations, either of reflected sunlight or intrinsic thermal emission, of the outer satellites of Jupiter are difficult to obtain because of the small size and great distance of these bodies. Probable errors in the data are consequently rather large. In spite of the intrinsic imprecision of infrared broadband color observations, such as JHKL, filter data are useful in determining colorimetric similarities among types of objects in the solar system. Figure 17 shows a JHK color plot of several small solar system objects. Asteroids of all types, C, S, and U, are clustered toward the top of the diagram, while icy satellites of Saturn and Jupiter occupy the lower left-hand region. The Uranian satellites, known to have icy surfaces (see below), cluster in a region between the Saturn satellites and the asteroids. While the data for J6 are crude (two conflicting observations are shown on the diagram, it seems clear that this object is more similar to asteroids than to icy satellites.

The Rings and Satellites of Saturn

The surface compositions of the particles in the main ring system of Saturn and the satellites have been determined from infrared spectrophotometry, spectroscopy, and photometry. The basic references to the discovery of water frost on the ring particles are Kuiper et al. (1970), Pilcher et al. (1970), and Clark (1980). The subject has been reviewed by Pollack (1975) and Cuzzi (1978). The presence of water frost/ice on the inner satellites was inferred by Johnson et al. (1975) and confirmed by Morrison et al. (1976) and Fink et al. (1976). Cruikshank (1979a) has reviewed the nature of the satellite system of Saturn, but some new information about Enceladus (S2), Iapetus (S8), and Phoebe (S9) has been obtained since that review was published.

The picture of the Saturn system of rings and satellites that emerges from the (largely infrared) data collected in the last decade is as follows: The brightest components of the rings show deep infrared absorption bands due to water frost, and laboratory simulations show that the frost is essentially pure with no significant admixture of silicate material (Clark 1980). The extended E ring is probably similarly composed of ice particles, but the observational data have not yet been completely interpreted. The bodies in the inner system of regular satellites (those in circular orbits of low inclination), of which three new members were discovered or confirmed during the 1980 ring-plane passage and the 1979 survey by the Pioneer 11 flyby, appear to be icy objects with surfaces covered completely with water frost or ice. Near-infrared spectroscopic data for S2 Enceladus, S3 Tethys, S4 Dione, and S5 Rhea show water ice absorptions clearly. Titan has a dense methane atmosphere which shows strong infrared absorptions of

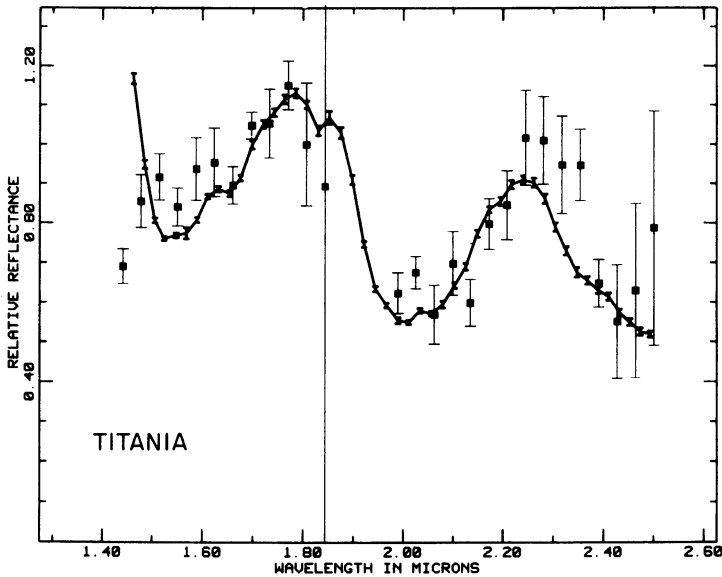


Figure 18. Spectrum of Titania (points with one-sigma error bars) compared with the spectrum of Ganymede (solid line). From Cruikshank (1980b).

variable strength. The observed variability suggests changes in the density of the aerosol haze in the atmosphere on a time scale of several hours. Emissions of methane and ethane are found in the mid-infrared spectrum of Titan, and the composition and mass of the satellite's atmosphere have been widely studied and speculated upon (Caldwell 1978; Hunten 1976, 1978). Beyond Titan, three satellites in non-circular and inclined orbits are known. S7 Hyperion appears to be an icy object (Cruikshank 1979b, 1980b), while S8 Iapetus is an icy body with its leading hemisphere (in the sense of the satellite's orbital motion around Saturn) covered by dark dust presumably of iron-bearing silicate material (Morrison et al. 1975; Cruikshank 1979a; Cruikshank et al. in preparation). A probable source of the dark material on the leading face of Iapetus is dust spiraling inward toward Saturn from S9 Phoebe, the irregular retrograde satellite exterior to Iapetus (Soter 1974; Cruikshank et al. in preparation; Degewij et al. 1980b). Phoebe's surface composition is not yet established with complete certainty, but the best colorimetric evidence in the photovisual region and in the near infrared (shown in Figure 17) suggests that its surface is comparable to that of dark asteroids rather than the icy inner satellites of Saturn. Phoebe is most likely a captured object of asteroidal character.

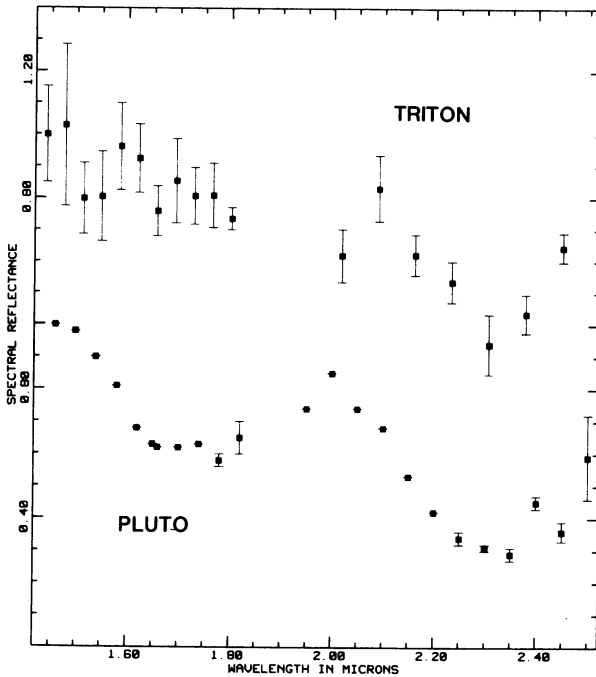


Figure 19. Spectra of Triton and Pluto showing absorptions attributed to methane gas (in the case of Triton) and methane frost (in the case of Pluto). The Triton data are adapted from Cruikshank and Silvaggio (1979) and those for Pluto from Soifer et al. (1980).

The Satellites and Rings of Uranus

Improvements in spectrometer sensitivity have made it possible to study the near-infrared spectra of the Uranian satellites with sufficient signal precision and spectral resolution to reveal the strong absorption bands at 2.0 and 2.4 μm characteristic of water ice/frost (Cruikshank 1980b; Cruikshank and Brown, 1980). JHK photometric observations (Cruikshank 1980b; Nicholson and Jones 1980) are consistent with this interpretation, and are shown in Figure 17. The spectrum of the outermost satellite, U4 Oberon, is shown in Figure 18 in comparison to the spectrum of Jupiter's Ganymede. Ganymede is known to have impurities of iron-bearing silicate material in its surface deposits of water frost, and because the depths of the ice absorption bands on Oberon are comparable to those on the Jovian satellite, Cruikshank (1980b) suggested that Oberon likewise has an impure surface layer of frost. Dynamical studies of the Uranian system (Greenberg 1975, 1976, 1978) together with the new infrared result, suggest that the bulk compositions of the satellites are dominated by water. To date, only the four largest satellites have been studied. The fact that the Uranian satellites lie in a field separate from Ganymede and the icy

satellites of Saturn in the JHK color plot (Figure 17) may indicate that the impurities in the frost are of different composition, or that the color of ice at the temperature of the Uranian satellites ($\sim 78\text{K}$) is different from that at the temperature of the Saturn satellites ($\sim 110\text{K}$).

While all four of the outer Uranian satellites show water frost absorption, the strength of the bands is not the same on all objects. In particular, U2 Umbriel has weaker absorption at $2\ \mu\text{m}$ than do the other satellites or Ganymede. Comparison with the spectrum of Callisto shows that the water frost bands are intermediate in strength between this satellite and Ganymede, suggesting that there is a larger fraction of impurities in the surface frost than on U1 Ariel, U3 Titania, and U4 Oberon. Umbriel is the faintest of the four large satellites, and it may be that the larger amount of dark impurities in the ice or frost results in a lower geometric albedo. None of the Uranian satellites can be resolved as disks from the Earth, and inferences as to their dimensions must presently be made on the basis of an assumed geometric albedo. The question of dimensions, mean densities, and masses is reviewed by Cruikshank (1980b).

The innermost known Uranian satellite, Miranda, has not been observed in the infrared because of its faintness ($m_V = 16.5$) and its proximity to the planet.

Unlike the rings of Saturn, the particles comprising the ring system of Uranus appear to be dark (Sinton 1977; Smith 1977). In the $2\text{-}\mu\text{m}$ spectral region where Uranus is very dark, Matthews et al. (1978) have obtained images of the Uranian ring system, though individual components are not resolved. Nicholson and Jones (1980) observed the reflectance spectrum of the rings in this same region and find marginal evidence for an absorption at $2.1\ \mu\text{m}$. The distinctive spectral signature of water ice or frost seen in the satellites is apparently not observed in the rings.

Triton and Pluto

Spectroscopy of Triton and Pluto in the photovisual spectral region (0.3 to $1.1\ \mu\text{m}$) has revealed only hints of absorptions attributable to atmospheres of methane evidenced by a suggestion of an absorption band at $8900\text{-}\text{\AA}$ (Benner et al. 1978). Until 1976, the infrared region, where most molecular absorptions are stronger than in the photovisual, had been neglected because of the faintness of the two bodies and the insensitivity of infrared detectors. Two-color photometric observations of Pluto (Cruikshank et al. 1976) suggested the presence of frozen methane through the strong absorption band at $1.7\ \mu\text{m}$ compared to $1.5\ \mu\text{m}$. Later spectrophotometry at 12 wavelengths between 1.44 and $1.84\ \mu\text{m}$ by Cruikshank and Silvaggio (1980) confirmed the presence of an absorption in the region of the strong band of methane, both gaseous and solid, while similar data for Triton in the region 1.44 and $2.52\ \mu\text{m}$ (19 points) showed a moderate absorption at $2.3\ \mu\text{m}$ and very little at $1.7\ \mu\text{m}$ (Cruikshank and Silvaggio 1979).

The presence of methane frost on Pluto was supported by filter photometry obtained by Lebofsky et al. (1979), but a spectrum of high quality in the region 1.46 - 2.46 μm by Soifer et al. (1980), reproduced in Figure 19, finally confirmed this interpretation by showing the strong frost absorption bands at 1.7 and 2.3 μm .

Cruikshank and Silvaggio (1980) reasoned that gaseous and solid methane cannot be distinguished from one another on Pluto with the existing data because their absorptions overlap. Because the absorptions at 1.7 μm and 2.3 μm are strong on Pluto, the presence of the solid material is assumed, and the presence of gaseous methane is inferred from vapor pressure considerations.

The coverage of solid methane on Pluto is not complete as evidenced by the downward slope toward the violet in the planet's photovisual reflectance spectrum. This behavior is suggestive of exposures or admixtures of silicate material with the ice or frost, as is the case with Europa and Ganymede.

The infrared data shown in Figure 19 for Triton are quite crude, especially in the 1.6- μm region, but show a distinct absorption centered at 2.3 μm attributed to gaseous methane. A new and improved spectrum obtained by Cruikshank (in preparation) in 1980 confirms the 2.3- μm absorption and reveals the 1.7- μm band as well. Cruikshank and Silvaggio (1979) consider the 2.3- μm absorption evidence of gaseous methane because of the relative weakness of the strong 1.7- μm absorption that would be expected for the solid form.

As with Pluto, the photovisual reflectance of Triton slopes down toward the violet, but it may be variable (Bell et al. 1979, Franz 1979). The slope implies the presence of silicate materials (Cruikshank et al. 1979) with no evidence for Rayleigh scattering at the shortest wavelengths.

The 2.3- μm absorption of methane on Triton was synthesized from laboratory data and a random absorption band model developed by Silvaggio (1977) with the result that for pure methane the surface column abundance is $(7 \pm 3) \times 10^2$ cm-agt, corresponding to a surface pressure of about $(1 \pm 0.5) \times 10^{-4}$ bars, a value consistent with the calculated vapor pressure of methane gas above methane ice at a temperature of 57-60 K. Thus, the vapor pressure considerations suggest that some frost is present on Triton, and Golitsyn (1979) has argued that most of the gas should be cold-trapped on the dark part of the satellite or toward the poles.

This work was supported in part by NASA grants NSG 7323, NSG 7312 and NGL 12-001-057.

REFERENCES

- Adams, J. B.: 1974, *J. Geophys. Res.*, 79, pp. 4829-4836.
- Adams, J. B., and McCord, T. B.: 1970, *Proceedings of the Apollo 11 Lunar Science Conference*, 3, pp. 1937-1945.
- Adams, J. B., and McCord, T. B.: 1972a, *Proceedings of the Third Lunar Science Conference*, 3, pp. 3021-3034.
- Adams, J. B., and McCord, T. B.: 1972b, *In Lunar Science III*, 1-3, Lunar Science Institute, Houston.
- Adams, J. B., and McCord, T. B.: 1973, *Proceedings of the Fourth Lunar Science Conference*, 1, pp. 163-177.
- Becklin, E. E., and Wynn-Williams, C. G.: 1979, *Nature*, 279, pp. 400-401.
- Bell, J. F., Clark, R. N., McCord, T. B., and Cruikshank, D. P.: 1979, *Bull. Am. Astron. Soc.*, 11, p. 570.
- Benner, D. C., Fink, U., and Cromwell, R. H.: 1978, *Icarus*, 36, pp. 82-91.
- Bowell, E., and Lumme, K.: 1979, in T. Gehrels (ed.), "Asteroids", Univ. of Arizona Press, Tucson, Arizona, pp. 132-169.
- Caldwell, J.: 1978, in D. M. Hunten and D. Morrison (eds.), "The Saturn system", NASA CP 2068, pp. 113-126.
- Chapman, C. R., and Gaffey, M. J.: 1979, in T. Gehrels (ed.), "Asteroids", Univ. of Arizona Press, Tucson, Arizona, pp. 655-687.
- Charette, M. P., McCord, T. B., Pieters, C., and Adams, J. B.: 1974, *J. Geophys. Res.*, 79, pp. 1605-1613.
- Clark, R. N.: 1980, *Icarus* (in press).
- Clark, R. N., and McCord, T. B.: 1980, *Icarus*, 41, pp. 323-339.
- Cruikshank, D. P.: 1979a, *Rev. Geophys. Space Phys.* 17, pp. 165-176.
- Cruikshank, D. P.: 1979b, *Icarus* 37, pp. 307-309.
- Cruikshank, D. P.: 1980a, *Icarus* 41, pp. 240-245.
- Cruikshank, D. P.: 1980b, *Icarus* 41, pp. 246-258.
- Cruikshank, D. P., and Brown, R. H.: 1980, *Bull. Am. Astron. Soc.* (in press).
- Cruikshank, D. P., Degewij, J., and Zellner, B.: 1981, in D. Morrison (ed.), "The Satellites of Jupiter", Univ. of Arizona Press, Tucson, Arizona (in press).
- Cruikshank, D. P., Jones, T. J., and Pilcher, C. B.: 1978, *Astrophys. J.*, 225, pp. L89-L92.
- Cruikshank, D. P., Pilcher, C. B., and Morrison, D.: 1976, *Science*, 194, pp. 835-837.
- Cruikshank, D. P., and Silvggio, P. M.: 1979, *Astrophys. J.*, 233, pp. 1016-1020.
- Cruikshank, D. P., and Silvggio, P. M.: 1980, *Icarus*, 41, pp. 96-102.
- Cruikshank, D. P., Stockton, A., Dyck, H. M., Becklin, E. E., and Macy, W., Jr.: 1979, *Icarus*, 40, pp. 104-114.
- Cuzzi, J.: 1978, in D. M. Hunten and D. Morrison (eds.), "The Saturn System", NASA CP 2068, pp. 73-104.
- Degewij, J., Andersson, L., and Zellner, B.: 1980a, *Icarus* (in press).
- Degewij, J., Cruikshank, D. P. and Hartmann, W. K.: 1980b, *Icarus*, (in press).

- Degewij, J., and van Houten, C. J.: 1979, In T. Gehrels (ed.), "Asteroids", Univ. of Arizona Press, Tucson, Arizona, pp. 417-435.
- Evans, D. L., and Adams, J. B.: 1979, Proc. Lunar Planet. Sci. Conf. 10th.
- Fanale, F. F., Brown, R. H., Cruikshank, D. P., and Clark R. N.: 1979, Nature, 280, pp. 761-763.
- Fink, U., Dekkers, N. H., and Larson, H. P.: 1973; Astrophys. J., 179, pp. L155-L159.
- Fink, U., Larson, H. P., Gautier, N., and Treffers, R.: 1976, Astrophys. J., 207, pp. L63-L67.
- Fink, U., Larson, H. P., Lebofsky, L. A., Feierberg, M., and Smith, H.: 1978, Bull. Am. Astron. Soc., 10, 580.
- Franz, Otto: 1979, private communication.
- Gaffey, M. J., and McCord, T. B.: 1977a, Tech. Rev., pp. 50-59.
- Gaffey, M. J., and McCord, T. B.: 1977b, Mercury, 6, pp. 1-9.
- Gaffey, M. J., and McCord, T. B.: 1978, Space Sci. Rev., 21, pp. 555-628
- Gaffey, M. J., and McCord, T. B.: 1979, in T. Gehrels, (ed.), "Asteroids", pp. 668-723.
- Gehrels, T., ed.: 1971, "Physical Studies of Minor Planets", NASA SP-267, Washington, DC, US Government Printing Office.
- Gehrels, T. (ed.): 1979, "Asteroids", Univ. of Arizona Press, Tucson, Arizona.
- Golitsyn, G. S.: 1979, private communication.
- Greenberg, R.: 1975, Icarus, 24, pp. 325-332.
- Greenberg, R.: 1976, Icarus, 29, pp. 427-433.
- Greenberg, R.: 1978, Bull. Am. Astron. Soc., 10, p. 585.
- Guinness, E. A., Arvidson, R. E., Gehret, D. C., and Bolef, L. K.: 1979, J. Geophys. Res., 84, pp. 8355-8364.
- Hapke, B., Danielson, G. E., Jr., Klaasen, K., and Wilson, L.: 1975, J. Geophys. Res., 80, pp. 2431-2443.
- Head, J. W., Adams, J. B., McCord, T. B., Pieters, C., and Zisk, S.: 1978, Proc. of the Conference on Luna 24 entitled "Mare Crisium: The View from Luna 24:", in R. B. Merrill and J. J. Papike (eds.), Pergamon Press, New York, pp. 43-74.
- Huck, J. O., Jobson, D. J., Park, S. K., Wall, S. D., Arvidson, R. E., Patterson, W. R., and Benton, W. D.: 1977, J. Geophys. Res., 82, pp. 4401-4411.
- Hunten, D. M.: 1976, in J. A. Burns (ed.), "Planetary Satellites", Univ. of Arizona Press, Tucson, Arizona, pp. 420-437.
- Hunten, D. M.: 1978, in D. M. Hunten and D. Morrison (eds.), "The Saturn System", NASA CP 2069, pp. 127-140.
- Johnson, T. V., Mosher, J. A., and Matson, D. L.: 1977a, Proc. Lunar Sci. Conf. 8th, pp. 1013-1028.
- Johnson, T. V., Saunders, R. S., Matson, D. L., and Mosher, J. A.: 1977b, Proc. Lunar Sci. Conf. 8th, pp. 1029-1036.
- Johnson, T. V., Veeder, G., and Matson, D. L.: 1975, Icarus, 24, pp. 428-432.
- Kuiper, G. P.: 1957, Astron. J., 62, p. 245.
- Kuiper, G. P., Cruikshank, D. P., and Fink, U.: 1970, Sky Telesc., 39, pp. 14 and 80.

- Larson, H. P., and Veeder, G. J.: 1979, in T. Gehrels, (ed.), "Asteroids", Univ. of Arizona Press, Tucson, Arizona, pp. 724-744.
- Lebofsky, L. A.: 1978, *Mon. Not. Roy. Astron. Soc.*, 182, pp. 17P-21P.
- Lebofsky, L. A., Rieke, G. H. and Lebofsky, M. J.: 1979, *Icarus*, 37, pp. 554-558.
- Matthews, K., Neugebauer, G., and Nicholson, P.: 1978, *Bull. Am. Astron. Soc.*, 10, p. 580.
- McCord, T. B.: 1968, California Institute of Technology, Pasadena, California (Ph.D. Thesis).
- McCord, T. B., and Adams, J. B.: 1972a, *Science*, 178, pp. 746-747.
- McCord, T. B., and Adams, J. B.: 1972b, *Icarus*, 17, pp. 585-588.
- McCord, T. B., Adams, J. B., and Johnson, T. V.: 1970, *Science*, pp.1445-1447.
- McCord, T. B., Charette, M. P., Johnson, T. V., Lebofsky, L. A., and Pieters, C.: 1972, *J. Geophys. Res.*, 77, pp. 1349-1359.
- McCord, T. B., and Clark, R. N.: 1979, *J. Geophys. Res.*, 84, pp. 7664-7668.
- McCord, T. B., and Clark, R. N., Hawke, B. R., McFadden, L. A., Owensby, P. D., Pieters, C. M., Adams, J. B.: 1980, *J. Geophys. Res.* (submitted).
- McCord, T. B., Clark, R. N., and Huguenin, R. L.: 1978, *J. Geophys. Res.*, 83, pp. 5433-5441.
- McCord, T. B., Grabow, M., Feierberg, M. A., MacLaskey, D., and Pieters, C.: 1979, *Icarus*, 37, pp. 1-28.
- McCord, T. B., Pieters, C., and Feierberg, M. A.: 1976, *Icarus*, 29, pp. 1-34.
- McCord, T. B., Singer, R. B., Clark, R. N.: 1980, *J. Geophys. Res.*, submitted.
- Moroz, V. I.: 1965, *Astron. Zh.* (in Russian), 42, pp. 1287-1295.
- Morrison, D., Cruikshank, D. P., Pilcher, C. B., and Rieke, G. H.: 1976, *Astrophys. J.*, 207, pp. L213-L216.
- Morrison, D., Jones, T. J., Cruikshank, D. P., and Murphy, R. E.: 1975, *Icarus*, 24, pp. 157-171.
- Nicholson, P. D., and Jones, T. J.: 1980, *Icarus*, 42, pp. 54-67.
- Pearl, J., Hanel, R., Kunde, V., Maguire, W., Fox, K., Gupta, S., Ponnampertuma, C., and Raulin, F.: 1979, *Nature*, 280, pp. 755-758.
- Pilcher, C. B., Ridgway, S. T., and McCord, T. B.: 1972, *Science*, 178, pp. 1087-1089.
- Pilcher, C. B., Chapman, C. R., Lebofsky, L. A., and Kieffer, H. H.: 1970, *Science*, 167, pp. 1372-1373.
- Pieters, C. M.: 1978, *Proc. Lunar and Plan. Sci. Conf.* 9th, pp. 2825-2849.
- Pieters, C. and McCord, T. B.: 1976, *Proc. Lunar Sci. Conf.* 7th, pp. 2677-2690.
- Pieters, C. M., Head, J. W., Adams, J. B., McCord, T. B., Zisk, S. H., and Whitford-Stark, J.: 1980, *J. Geophys. Res.*, 85, pp. 3913-3938.
- Pollack, J. B.: 1975, *Space Sci. Rev.*, 18, pp. 3-94.
- Rieke, G. H.: 1975, *Icarus*, 25, pp. 333-334.
- Rose, H. J., Jr., Baedeker, P. A., Berman, S., Christian, R. P., Dwornik, E. J., Finkelman, R. B., and Schnepfe, M. M.: 1975, *Proc. Lunar Sci. Conf.* 6th, 2, pp. 1362-1373.

- Sill, G. T., and Clark, R. N.: 1981, in D. Morrison (ed.), "The Satellites of Jupiter", Univ. of Arizona Press, Tucson (in press).
- Silvaggio, P. M.: 1977, Cornell Univ. Ithaca, New York (Ph.D Thesis).
- Singer, R. B., McCord, T. B., Clark, R. N., Adams, J. B., and Huguenin, R. L.: 1979, *J. Geophys. Res.*, 84, pp. 8415-8426.
- Sinton, W. M.: 1977, *Science*, 198, pp. 503-504.
- Smith, B. A.: 1977, *Nature*, 268, p. 32.
- Smith, D. W., Johnson, P. E., and Shorthill, R. W.: 1981, *Icarus*, (submitted).
- Soderblom, L. A., Edwards, K., Eliason, E. M., Sanchez, E. M., and Charette, M. P.: 1978, *Icarus*, 34, pp. 446-464.
- Soifer, B. T., Neugebauer, G., and Matthews, K.: 1980, *Astron. J.*, 85, pp. 166-167.
- Soter, S.: 1974, paper presented at IAU Colloquium 28, Ithaca, New York.
- Strickland, E. L., III.: 1979, in *Lunar and Plan. Sci. X*, Lunar and Planetary Institute, Houston, Texas, pp. 1192-1194.
- Taylor, S. R.: 1975, "Lunar Science: A Post-Apollo View", Pergamon, New York.
- Tepper, L., and Hapke, B.: 1977, *Bull. Am. Astron. Soc.*, 9, p. 532.
- Thomas, P., and Veverka, J.: 1981, in D. Morrison (ed.), "The Satellites of Jupiter", University of Arizona Press, Tucson, Arizona, (in press).
- Vilas, F., and McCord, T. B.: 1976, *Icarus*, 28, pp. 593-599.

DISCUSSION FOLLOWING PAPER DELIVERED BY T. B. MCCORD

ALLEN: The only asteroid you mentioned was Vesta which, I believe, has an unusual surface. Can you mention what you find on other asteroids, if they've been observed?

MCCORD: We find a wide variety of surface compositions among the asteroids. A few percent of the total sample have surfaces composed of metals, but many are dominated by olivine and pyroxene. A large fraction of the objects appear similar to carbonaceous chondritic material. There are many subtle subdivisions in the compositional classification of asteroids which have been extensively reviewed in the literature, for example by Gaffey and McCord in the book Asteroids edited by T. Gehrels, 1979, University of Arizona Press.